Dalton Transactions

ROYAL SOCIETY OF CHEMISTRY

PAPER

View Article Online
View Journal | View Issue

Cite this: *Dalton Trans.*, 2025, **54**, 12454

Development of super-heat-resistant purine-based coordination polymers for applications in energetic materials†

Qamar-un-Nisa Tariq,[a,b] Maher-un-Nisa Tariq,[c] Saira Manzoor,[a,b] Qiyao Yu *[b] and Jian-Guo Zhang *[b]

Recent studies highlight the potential of nitrogen-rich, high-energy coordination polymers (CPs) for the development of next-generation energetic materials. Compared to traditional organic explosives, they provide improved density, sensitivity, oxygen balance, and heat of detonation. However, the tuning of high-energy CPs with respect to their energetic properties and the decoding of their structure–function relationship are still in the nascent phase. This work highlights the role of coordination polymerization in tailoring key energetic and physicochemical properties, including density, mechanical insensitivity, and thermal stability. Purine (a naturally occurring and widely available ligand) was used to synthesize two energetic coordination polymers (ECPs): **ECP-1** $[Ag(L_1)(ClO_4)_2]_n$ and **ECP-2** $[Ag(L_2)(NO_3)_2]_n$. Crystal structure analysis revealed that **ECP-1** forms a wavelike three-dimensional network, while **ECP-2** exhibits a solvent-free compact lamellar 3D structure. Both ECPs exhibit excellent thermal stability (T_d = 320.4–405.2 °C) with significantly improved densities (2.36–2.37 g cm^{-3}), acceptable detonation velocities (6707–7691 m s^{-1}) and detonation pressures (22.5–32 GPa), while being insensitive to mechanical stimuli (IS = 40 J; FS = 360 N). Additionally, this study provides a pathway for synthesizing novel ECPs based on naturally occurring ligands with dual structures, promoting a balance between energetic performance and safety while offering versatile functionality.

Received 26th June 2025,
Accepted 22nd July 2025

DOI: 10.1039/d5dt01509j

rsc.li/dalton

1. Introduction

The demands of contemporary research involve developing and synthesizing the next-generation energetic materials (EMs)[1] that exhibit high density,[2] excellent thermal stability,[3] and insensitivity to mechanical stimuli.[4] These materials are crucial for both civil[5] and military applications.[6] The EMs are categorized into three main types based on their applications: pyrotechnics, propellants, and high explosives. The major types of EMs can be subdivided into the following categories: (i) primary explosives,[7,8] (ii) secondary explosives (high explosives),[9] (iii) smoke-producing munitions (pyrotechnics),[10] (iv) decoyflares (pyrotechnics),[11] (v) igniters and detonators (pyrotechnics),[12] (vi) light-generating pyrotechnics (pyrotechnics),[13] (vii) gun propellants (propellants),[14] and (viii) rocket propellants (propellants).[15]

The detonation properties (velocity and pressure) are directly influenced by the density of a material, as higher density tends to boost the power of an explosive.[16,17] Additionally, insensitivity towards thermal and mechanical stimuli (impact and friction) is a key factor in the safe synthesis and handling of EMs.[18] Advanced EMs with improved physicochemical and energetic properties (such as thermal and mechanical stability, density, detonation velocity, and pressure) can be achieved by synthesizing new molecules[19] or slightly modifying the already known compounds.[20] Researchers have made numerous contributions to resolving the conflict between sensitivity and energetic properties. Emerging approaches such as salt formation,[21] co-crystallization,[20] coordination polymerization,[22] and synthesis of metastable interstitial composites (MICs)[23] are providing new insights that are not readily achievable through simple organic synthesis. Over the past few years, high-energy coordination polymers (CPs)[24] have gained a lot of attention as

[a]*International Collaborative Laboratory of 2D Materials for Optoelectronics Science and Technology of Ministry of Education, Institute of Microscale Optoelectronics, Shenzhen University, Shenzhen, 518060 China*
[b]*State Key Laboratory of Explosion Science and Technology, Beijing Institute of Technology, Beijing, 100081, China. E-mail: zjgbit@bit.edu.cn, qiyaoyu@bit.edu.cn*
[c]*School of Electrical and Information Engineering, Tianjin University, Tianjin 300072, China*

†Electronic supplementary information (ESI) available: X-ray crystallographic data for ECPs (**1** and **2**), including its bond lengths [Å], bond angles [°], torsion angles [°], and hydrogen bonding information; as well as FTIR spectra of ECPs (**1** and **2**). CCDC 2429086 and 2429111. For ESI and crystallographic data in CIF or other electronic format see DOI: https://doi.org/10.1039/d5dt01509j

next-generation EMs. Due to their structural ability, compact packing modes, intriguing architectures, and high mechanical strength.[25] Nonporous CPs with a high heat of formation and superior density have the potential to serve as EMs.[25] Energetic coordination polymers (ECPs) have gained significant interest and have become a focal point for researchers owing to their distinct structures and exceptional performance. Within the domain of EMs, ECPs have unique structural features and diverse applications in various energetic fields, including pyrotechnics, propellants, primary and secondary explosive formulations.[26] The design of ECPs can be tailored through careful selection of ligands, the nature and number of metal ions, and the incorporation of external anionic species.[27]

The synthesis of ECPs containing protonated ligands, metals, and anions is one of the most challenging tasks.[26] The presence of additional external anions as oxidizing agents in ECPs significantly improves both the reaction rate and the energetic properties. Oxidizing groups are introduced at the molecular level *via* self-assembly or self-crystallization methods.[28] The sensitivity and thermal stability of ECPs can be tailored by varying the metal ions or organic linkers. Owing to the lack of established structure–activity relationships, the ability to tune the thermal stability of organic linkers by forming the CPs remains a promising approach for further exploration. At present, a new combination method is urgently needed to break through the development challenges of ECPs (Fig. 1).

As far as we are aware, there is no existing literature that explores the ECPs of adenine and 2,4-diamino purine for modulating the energetic properties of the material. The naturally occurring fused heterocyclic derivatives (purines) possess strong electron-donating effects, and their distinctive spatial arrangement allows the construction of a stable eight-membered ring through coordination with central metal ions, making them highly suitable ligands. In this study, we have strategically employed two ionizable fused rings (leveraging the numerous nitrogen-donor sites of purines) to form coordination bonds with transition metal (silver) ions, producing high-energy-density materials (HEDMs) that exhibit excellent thermal stability. Different combinatorial methods facilitate the inclusion of more oxidants in the molecular structure, directly influencing the energetic properties of CPs. Both of these ECPs have incorporated oxidizing functionalities at the

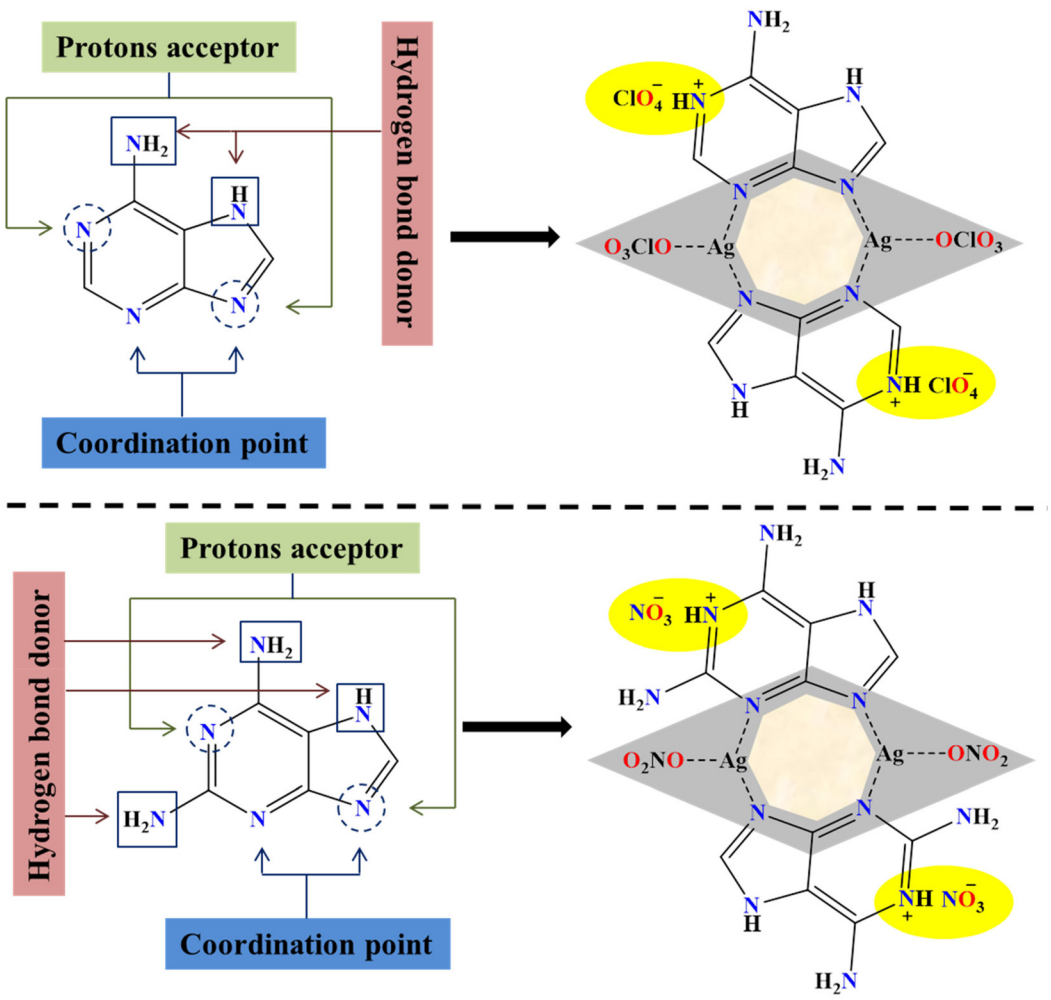

Fig. 1 A schematic illustration of **ECP-1** and **ECP-2**.

molecular scale through an effective self-assembly method. Additionally, they exhibit a dual structure composed of CPs and ionic salts. Both ECPs display identical coordinating behavior, establishing a strong basis for subsequent exploration. The structure of ECPs (**1** and **2**) was determined through Fourier-transform infrared spectroscopy (FT-IR), elemental analysis (EA), and single-crystal X-ray diffractometry, and their thermal decomposition behavior was analyzed using differential scanning calorimetry (DSC). The exceptional thermal and mechanical stability of these newly synthesized ECPs is likely attributed to their distinct structures. A combination of experimental techniques and theoretical modeling was used to comprehensively explore the structure–activity relationship.

2. Materials and methods

Caution! The prepared ECPs (**1** and **2**) are hazardous, so it is crucial to handle them with care. We did not encounter any explosions during the synthesis and testing of these ECPs. During the handling and storage of both ECPs, scarping and scratching should be avoided. Additionally, we strongly recommend conducting small-scale experiments while following proper safety protocols (Kevlar gloves, thick leather coat, wrist protectors, ear plugs, and a face shield) to minimize the risk of accidental explosions or possible injuries.

2.1. Materials and reagents

The two purine compounds (9*H*-purine-6-amine (L_1) and 9*H*-purine-2,6-diamine (L_2)) were used without any further purification after purchasing from Aladdin. All chemicals and reagents, including metal salts and solvents were purchased from Sigma-Aldrich and Aladdin, supplied as analytical grade, and used without additional treatment.

2.2. Characterization methods

The infrared (IR) spectra were obtained using a Thermo Nicolet iS10 spectrometer, fitted with a Thermo Scientific Smart iTR diamond ATR accessory. The thermal decomposition behavior of prepared ECPs was analyzed using differential scanning calorimetry (DSC) with a heating rate of 10 °C min^{-1}. The DSC 3 equipment (Mettler Toledo) was used for the thermal analysis, conducted from room temperature to 500 °C under a nitrogen atmosphere, with a flow rate of 50 mL min^{-1}. A Vario EL III C, H, N elemental analyzer was used to perform the elemental analysis. The experimental density was measured using the powder densitometer (Micromeritics AccuPyc II 1340). The mechanical sensitivities of the ECPs, including both friction and impact sensitivity, were measured using the standard BAM methods. Impact sensitivity was determined by using a BAM BFH-10 drop weight device, equipped with a 10 kg drop weight. Friction sensitivity was determined by using BAM friction apparatus FSKM-10.

Single-crystal X-ray diffraction of the prepared ECPs was carried out using a Bruker CCD area detector diffractometer, using graphite-monochromatized Mo Kα radiation (λ = 0.71073 Å) with phi and omega scans. Data collection and initial cell refinement were performed using the BRUKER SMART system, SHELXS-97[29] and SHELXL-97[30] programs were used to further solve and refine the structures. The full-matrix least-squares approach of F^2 was employed to determine the thermal parameters and atomic coordinates of each non-H atom. Anisotropic refinement was applied to the non-H atoms, while the H atoms were treated using a riding model. The crystal structure, hydrogen bonding (intra- and intermolecular), and three-dimensional packing were analyzed using Diamond software (version 3.2 K).

2.3. Synthesis of ECP-1

L_1 (9*H*-purine-6-amine, 1 mmol) was completely dissolved in 10 mL of water at 80–85 °C. An aqueous solution of silver perchlorate salt (1 mmol, pre-dissolved in 10 mL of water) was added gradually, and the reaction mixture was stirred for 30 min. White precipitates were initially formed; upon heating, $HClO_4$ was added dropwise until the mixture turned clear (Scheme 1). The resulting solution was filtered and left to evaporate slowly at low temperature (5–10 °C). After one week, block-shaped crystals (**ECP-1·H_2O**) suitable for single-crystal X-ray diffraction measurement were obtained. **ECP-1** was obtained by drying the **ECP-1·H_2O** sample at 48 h at 40 °C in a vacuum oven containing P_2O_5.

Yield: 80%. DSC (10 °C min^{-1}): 320.4 °C (*exo*). IR (ν, cm^{-1}): 3390, 3125, 2922, 2360, 1700, 1653, 1605, 1507, 1416, 1308, 1240, 1079, 939, 895, 716, 640, 628. EA (%) calcd for $C_{10}H_{15}Cl_4Ag_2N_{10}O_{17}$ (903.85 g mol^{-1}); C 13.29, H 1.56, N 15.50; found: C 13.28, H 1.57, N 15.51.

2.4. Synthesis of ECP-2

1 mmol of L_2 (9*H*-purine-2,6-diamine) was completely dissolved in 10 mL of water at 80–85 °C. Subsequently, an aqueous solution of silver nitrate salt (1 mmol of salt, pre-dissolved in 10 mL of water) was gradually added, and the reaction mixture was allowed to proceed for 30 min (Scheme 1). The white solid formed, and with continuous heating, HNO_3

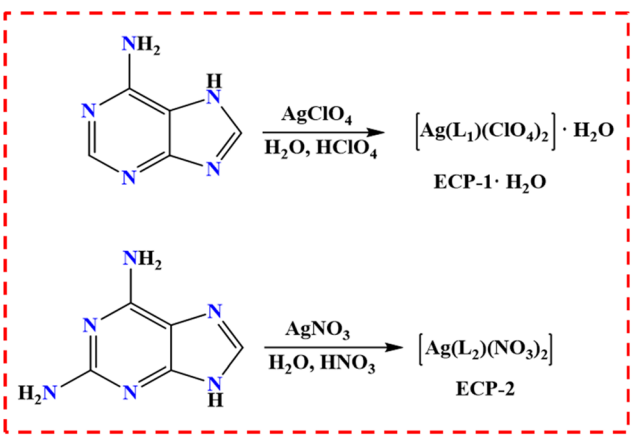

Scheme 1 Synthesis scheme of the **ECP-1·H_2O** and **ECP-2**.

was added dropwise until the solution became clear. After filtration, the clear filtrate was allowed to evaporate slowly at a low temperature (5–10 °C). After 3 to 4 days, needle-shaped crystals suitable for single-crystal X-ray diffraction measurement were formed.

Yield: 81%. DSC (10 °C min^{-1}): 216.7 °C (onset), 405.2 °C (*exo*). IR (ν, cm^{-1}): 3388, 3126, 2898, 1705, 1647, 1572, 1458, 1385, 1295, 1240, 1105, 1047, 956, 856, 796, 717, 684, 661. EA (%) calcd for $C_{10}H_{14}Ag_2N_{16}O_{12}$ (766.11 g mol^{-1}); C 15.68, H 1.84, N 29.26; found: C 15.66, H 1.85, N 29.28.

3. Results and discussion

3.1. Synthesis

In this study, purines were used as polydentate ligands to react with Ag(I) salts, which exhibit unique coordination capabilities, to prepare these two ECPs (**1** and **2**) having the same dimensions. Purines (L_1 and L_2) were fully dissolved in water (10 mL) at 80–85 °C. After that, a 1 mmol aqueous solution of silver salt ($AgClO_4$ or $AgNO_3$) was added gradually, and the reaction mixture was stirred for 30 min, leading to the formation of white precipitates. The formation of a considerable amount of white solid is ascribed to the high coordination ability of Ag(I). The corresponding acid ($HClO_4$ or HNO_3) was introduced dropwise with heating until the solution became transparent. The anion also influences the polymerization ability of purines and Ag(I). The perchlorate ion group is more favorable for forming compact ECP; more $HClO_4$ is needed to dissolve them. This process is termed the 'dissolution and crystallization of ECPs powder'.

After evaporation at a low temperature (5–10 °C) for several days, suitable crystals for X-ray analysis were obtained from the transparent solution. Scheme 1 provides an overview of the synthetic strategy of **ECP-1** and **ECP-2**.

3.2. Single-crystal X-ray diffraction analysis

The single-crystal X-ray diffraction analysis of **ECP-1·H_2O** was conducted using a crystal of appropriate size (0.35mm × 0.26mm × 0.10 mm). **ECP-1·H_2O** crystallize in the monoclinic crystal system with the $P2_1/c$ space group and possess a density of 2.36 g cm^{-3} (293 K). The structure of **ECP-1·H_2O** contains two molecules in the unit cell (Z = 2), and its empirical formula is $C_{10}H_{16}Cl_4Ag_2N_{10}O_{18}$ (Table 1). Through sp hybridization, Ag^+ is forming a bidentate coordination with a purine polydentate ligand (using the N atoms, as illustrated in Fig. 2) and with the acid ion through its O atom. The crystal structure of **ECP-1·H_2O** contains two molecules of an adenine ligand, two silver cations, two crystallized water molecules, and four perchlorate ions groups (two are coordinated (Ag–O1 2.620(5) Å), and two are non-coordinated). In purine, a six-membered ring is fused with five-membered ring, and protonation occurs at the nitrogen atom (N4) of the six-membered ring. Each silver ion forms coordination bonds with the N1 and N3 nitrogen atoms of two different adenine molecules and the oxygen atom of the bridging perchlorate, resulting in a distorted trigonal pyramidal geometry. The distance between Ag···Ag is 2.9845(9) Å, indicating a significant argentophilic interaction. The bond distance between silver and oxygen (Ag1–O1 = 2.62(5) Å) is longer than the silver–nitrogen bond distances (Ag1–N1 = 2.147(4) Å and Ag1–N3 = 2.191(4) Å).

Table 1 X-ray Crystallographic information and refinement of **ECPs 1** and **2**

Parameters	**ECPs-1**	**ECPs-2**
Formula	$C_{10}H_{16}Ag_2Cl_4N_{10}O_{18}$	$C_{10}H_{14}Ag_2N_{16}O_{12}$
Formula mass	921.87	766.11
Temperature (K)	293	298
Crystal system	Monoclinic	Triclinic
Space group	$P2_1/c$	$P\bar{1}$
Z	2	1
a (Å)	14.9082(13)	6.1409(5)
b (Å)	7.3235(8)	7.4061(7)
c (Å)	12.9223(11)	12.8931(11)
α	90	86.286(3)
β	112.973(5)	89.118(3)
γ	90	66.436(2)
Cell volume (Å^3)	1299.0(2)	536.32(8)
Crystal color	Colorless	Colorless
Crystal shape	Block	Needle
d (g cm^{-3})	2.36	2.37
Size (mm)	0.35 × 0.26 × 0.10	0.17 × 0.08 × 0.05
F (000)	904	376
Reflections θ (°)	2.97–25.02	3.01–25.01
h	−14 to 17	−7 to 7
k	−8 to 8	−8 to 6
l	−15 to 15	−15 to 12
Number of unique reflections	5927	2604
Number of observed reflections	2281	1846
R_{int}	0.0443	0.0381
R_1, wR_2[$I > 2\sigma(I)$]	0.0418, 0.1081	0.0583, 0.1633
R_1, wR_2[all date]	0.0491, 0.1117	0.0651, 0.1683
CCDC	2429086	2429111

Fig. 2 illustrates the crystal structure, hydrogen bonding, three-dimensional (3D) packing, and a simplified diagram of the crystal stacking of **ECP-1·H_2O**. The atomic numbering is indicated in Fig. 2(a). Strong hydrogen bonds (intramolecular and intermolecular) stabilize the crystal packing and build the 3D network. As shown in Fig. 2(b), the **ECP-1·H_2O** features prominent inter- and intramolecular hydrogen bonding interactions (O–H···O, N–H···O, and N–H···Cl), resulting in layers that are stacked in a waveform pattern.

Single-crystal X-ray diffraction analysis of **ECP-2** was carried out by selecting a suitably sized crystal (0.17 mm × 0.08 mm × 0.05 mm). It exhibits a triclinic crystal structure with a crystal density of 2.37 g cm^{-3} (298 K) and belongs to the $P\bar{1}$ space group. The structure of **ECP-2** contains one molecule per unit cell (Z = 1), and its empirical formula is $C_{10}H_{14}Ag_2N_{16}O_{12}$. Its crystal structure contains two 9*H*-purine-2,6-diamine ligands, two silver cations, and four nitrate ion groups; two of the nitrate ions are coordinated (Ag–O1 = 2.60(10) Å), and two are non-coordinated. Although water was used as the solvent, the crystal structure confirms the absence of solvent molecules (Fig. 3). Similar to **ECP-1·H_2O**, the nitrogen atom in the six-

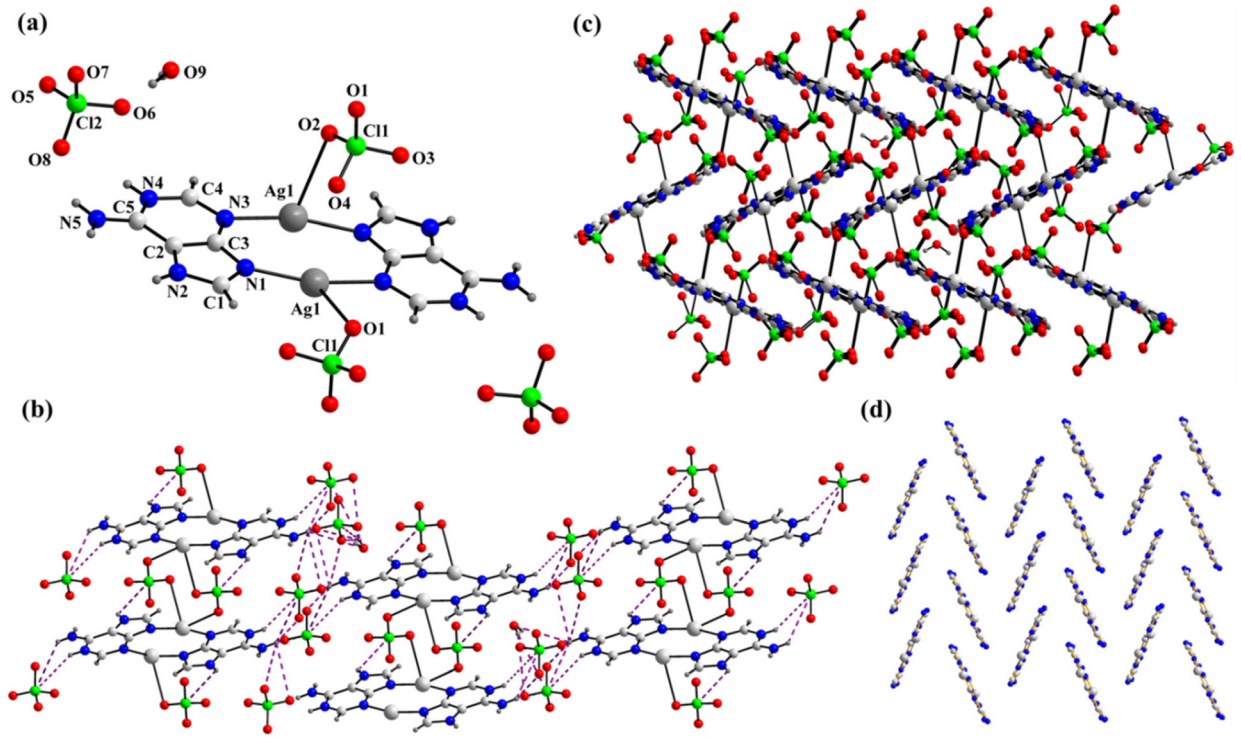

Fig. 2 (a–d) Labeled crystal structure, inter- and intramolecular hydrogen bonding network (indicated by purple dotted lines), 3D crystal packing, and a simplified diagram for crystal stacking of **ECP-1·H_2O**.

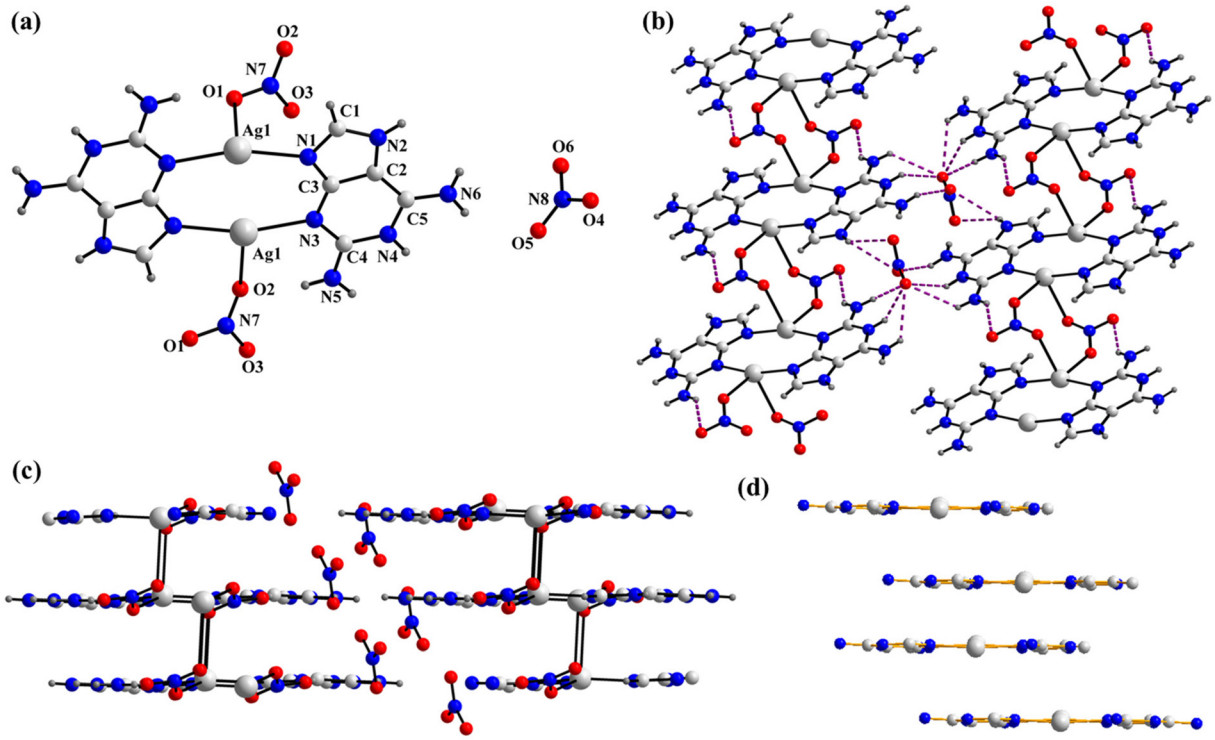

Fig. 3 (a–d) Labeled crystal structure, inter- and intramolecular hydrogen bonding network (represented by purple dotted lines), 3D crystal packing, and a simplified diagram for crystal stacking in **ECP-2**.

membered ring (N4) is protonated. Each silver ion is coordinated with the N1 and N3 atoms of two different 9*H*-purine-2,6-diamine molecules and oxygen of the bridging nitrate, resulting in a distorted trigonal pyramidal geometry. The distance between Ag1–O1 (2.60(10) Å) is longer than that of Ag1–N1 (2.184(6) Å) and Ag1–N3 (2.204(6) Å). The crystal structure, hydrogen bonding interactions, and three-dimensional (3D) packing arrangements of **ECP-2** are shown in Fig. 3. The atomic numbering is labeled in Fig. 3(a). The potent intramolecular/intermolecular hydrogen bonds (N–H···O) serve to stabilize the three-dimensional packing (Fig. 3(c)). The layers are stacked in a compact lamellar form.

3.3. Hirshfeld surface analysis

To explore the interactions within the crystal structures of this series of closely related molecules, Hirshfeld surface analysis[31] was performed, and their 2D fingerprint plots[32] were produced using Crystal Explorer 17.5 software.[33]

The Hirshfeld surface analysis provides a quantitative approach to studying intermolecular interactions in molecules, while 2D fingerprint plots serve as an effective tool for analyzing the crystal structure. The 2D fingerprint plot (derived from the Hirshfeld surface) provides a graphical depiction of the frequency distribution of different d_i and d_e combinations across the surface of the molecule. Numerous distinct points on the molecular Hirshfeld surface contribute to the generation of the 2D fingerprint plot. The values of d_i and d_e for each point provide information on relative distance; smaller (d_i + d_e) values correspond to the dense packing of atoms. The Crystal Explorer 17.5 program[33] was employed to study the Hirshfeld surfaces[34] of **ECP-1·H$_2$O** and **ECP-2**, and the resulting data are presented in Fig. 4a and b.

Fig. 4a and b provide a visual depiction of the seven most significant atomic contacts contributing to the Hirshfeld surface of **ECP-1·H$_2$O** and **ECP-2**. Notably, the O–H/H–O hydrogen bonds are the key atomic interactions occurring between two different molecules. Moreover, the 2D fingerprint plots clearly highlight the O–H interactions as sharp peaks, reflecting their relatively shorter contacts compared to other interactions such as C–O, H–H, and O–O. The total percentage of hydrogen bonding (O–H and N–H) is significantly higher than that of other atomic interactions like the C–C, N–N, C–N, or C–H bonds. The O–H and N–H interactions account for 50.4% in

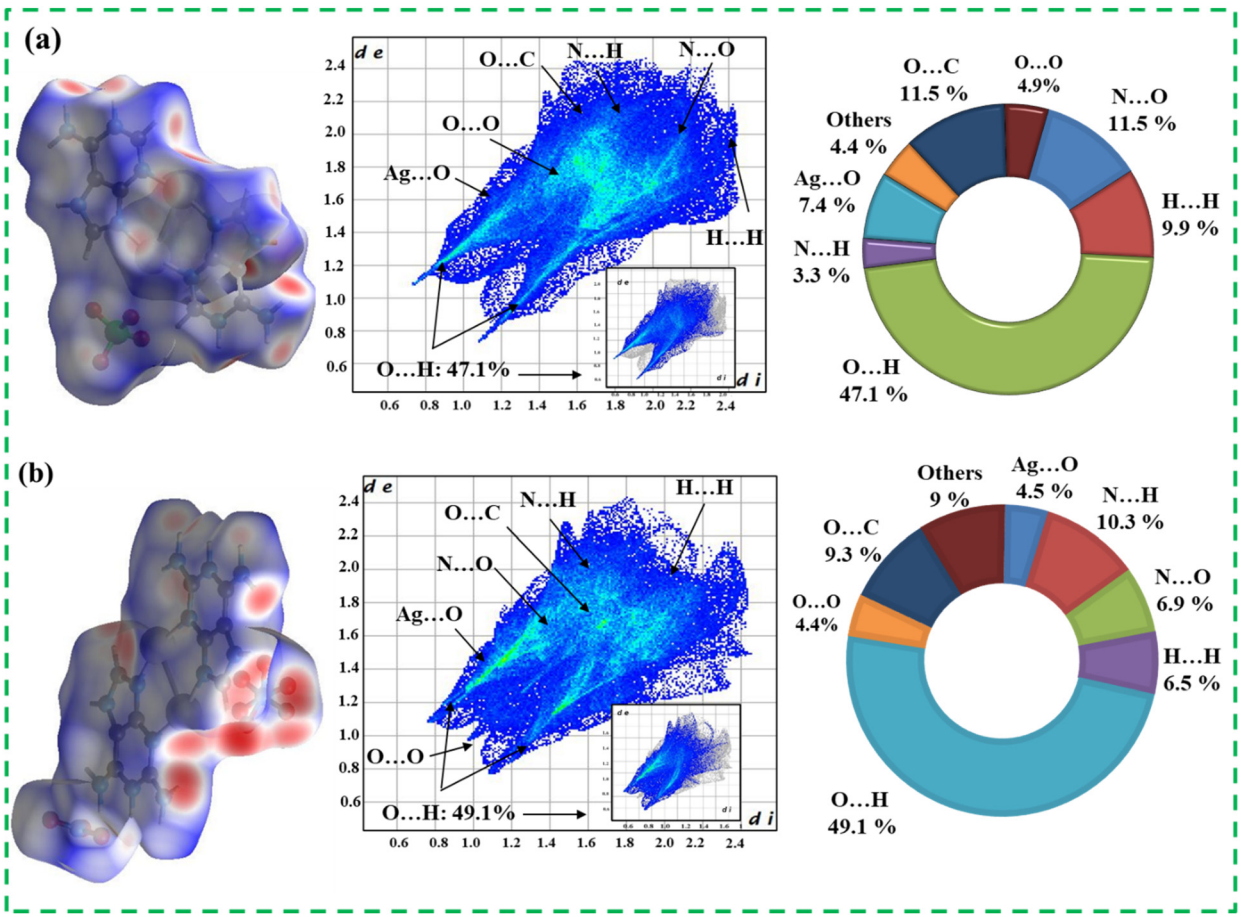

Fig. 4 (a and b) Hirshfeld surface analysis, 2D fingerprint plots, and individual atomic contact percentage contributions to the Hirshfeld surface of **ECP-1·H$_2$O** and **ECP-2**.

ECP-1·H_2O and 59.4% in **ECP-2**, suggesting that hydrogen bonding plays a crucial role in stabilizing the crystal structure of both **ECP-1·H_2O** and **ECP-2**.

3.4. Thermal stability

Thermal stability is an important parameter for evaluating the performance of EMs because it directly affects their transportation, storage, and applications. Differential scanning calorimetry (DSC) was used to study the thermal decomposition behavior of both ECPs (**ECP-1** and **ECP-2**) at a heating rate of 10 °C min^{-1}.

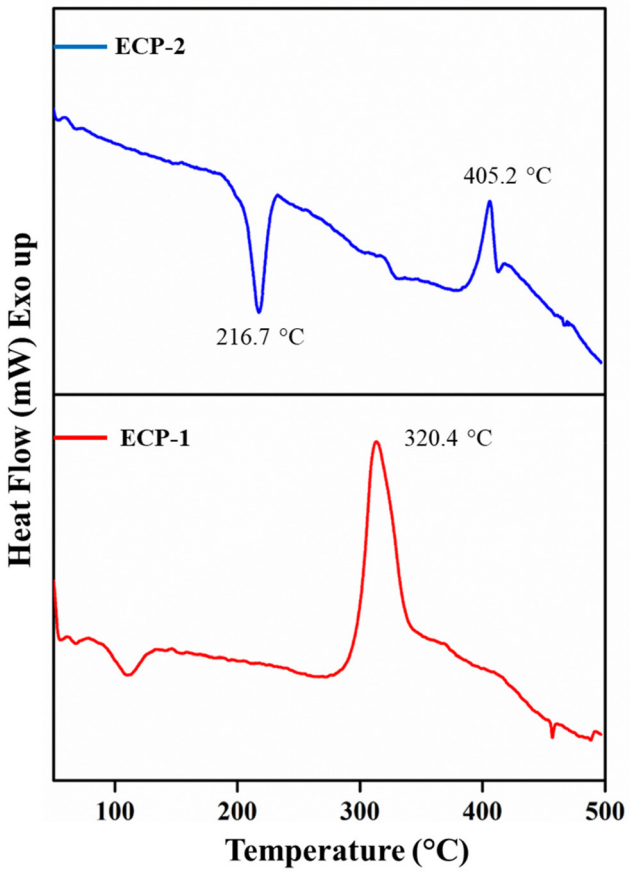

Fig. 5 The DSC curves of **ECP-1** and **ECP-2**.

In the initial stage, **ECP-1** undergoes decomposition without melting at 310.3 °C, attaining a peak temperature of 320.4 ± 1.7 °C. Meanwhile, **ECP-2** starts melting at 210.8 °C, reaching a peak temperature of 216.7 ± 1.3 °C. **ECP-2** exhibits high melting and decomposition temperatures and begins to decompose at 395 °C. The exothermic decomposition peak appears slightly broad, and the optimum temperature is 405.2 ± 1.5 °C (Fig. 5). Both synthesized ECPs exhibit excellent thermal stability and have high decomposition temperatures.

3.5. Energetic properties and safety test

The safety and energetic properties are two important factors for the performance evaluation of EMs. In this study, data on the physicochemical and energetic performances were evaluated and presented in Table 2. The density measurement of **ECP-1** and **ECP-2** at ambient temperature was obtained using a densitometer. Before testing, the sample was subjected to vacuum drying at 40 °C for 48 hours to ensure complete removal of crystallized water. Both **ECP-1** (2.36 g cm^{-3}) and **ECP-2** (2.37 g cm^{-3}) exhibited higher densities. The EXPLO5 (v6.04) program[35] was employed to determine the detonation properties of both ECPs, considering their experimental densities (at room temperature) and standard molar enthalpies of formation. Both **ECP-1** and **ECP-2** possess better detonation properties, with detonation velocities of 7691 m s^{-1} and 6707 m s^{-1} and corresponding detonation pressures of 32 GPa and 22.5 GPa, respectively. The detonation performance of the prepared **ECP-1** is significantly better than that of the reference compounds ($[Ag(IZ\text{-}4\text{-}CA)ClO_4]_n$, $[Ag(4\text{-}PZCA)ClO_4]_n$, $[Ag(3\text{-}HPZCA)_2(ClO_4)_3]_n$, and $[Ag_2(BNOD)\cdot(DMF)_2]_n$).

The safety profile of these ECPs was assessed by experimentally determining their thermal stability and mechanical sensitivity. The inherent contradiction between high energy and stability makes it challenging to achieve both in a single compound. In the case of prepared ECPs (**1** and **2**), we tried our best to strike a good balance. These ECPs (**1** and **2**) have higher decomposition temperatures than the reference compounds.[36–40]

Sensitivity directly influences the safe and reliable use of EMs in practical applications. Initial safety testing involved measuring the impact sensitivity (IS) and friction sensitivity (FS) of **ECP-1** and **ECP-2**, following the corresponding BAM standard procedure. The impact sensitivity was measured with

Table 2 Physicochemical and energetic properties of ECPs and reference EMs

No.	d^a (g cm^{-3})	D^b (m s^{-1})	P^c (GPa)	HOF^d (kJ mol^{-1})	T_d ^{e} (°C)	IS^f (J)	FS^g (N)
ECP-1	2.36	7691	31.97	73.72	320.4	>40	>360
ECP-2	2.37	6707	22.49	−610.0	405.2	>40	>360
$[Ag(IZ\text{-}4\text{-}CA)ClO_4]_n$ [36]	2.46	6300	22.4	—	210	21	80
$[Ag(4\text{-}PZCA)ClO_4]_n$ [37]	2.48	6100	20.1	—	260	5	9
$[Ag(3\text{-}HPZCA)_2(ClO_4)_3]_n$ [38]	2.09	7300	27.1	—	258	13	40
$[Ag_2(BNOD)\cdot(DMF)_2]_n$ [39]	2.17	7141	24.10	—	200	12	180
RDX[40]	1.82	8795	34.9	86.3	205	5.8	120

[a] Density. [b] Calculated detonation velocities. [c] Calculated detonation pressure. [d] Heat of formation. [e] Temperature of decomposition. [f] Impact sensitivity. [g] Friction sensitivity.

a standard BAM fall hammer, while friction sensitivity was assessed using a BAM friction tester. Both ECPs exhibit insensitivity to mechanical stimuli (IS: 40 J; FS: 360 N), which is attributed to their compact 3D stacking, stabilized by numerous inter- and intramolecular hydrogen bonds. The insensitivity of both ECPs is influenced by hydrogen bonding as well as the presence of $-NH_2$ groups. The findings indicate that both ECPs can be classified as thermally stable and insensitive advanced EMs.

4. Conclusions

The energetic coordination polymers (ECPs) offer a valuable approach due to their simple and straightforward synthesis and the broad range of possible combinations of ligands, metals, and anions. Two novel ECPs based on 9*H*-purin-6-amine and 9*H*-purine-2,6-diamine ligands were prepared in order to investigate their energetic and physicochemical properties using a coinage metal (Ag^+) and two distinct anions (perchlorate and nitrate). In addition to structural elucidation through X-ray diffraction, DSC, FTIR, EA, and standard sensitivity measurements (impact and friction) were conducted to accurately determine how coordination chemistry influences the energetic properties of these ECPs. Additionally, the detonation properties (D = 6707–7691 m s^{-1}, P = 22.5–32 GPa) of these ECPs were determined using the EXPLO5 6.04 program. A lower number/absence of water content, as well as the incorporation of nitrate/perchlorate ligands, led to an incredible increase in thermal and mechanical stability. Both ECPs possess higher densities (2.36–3.37 g cm^{-3}), while **ECP-1** exhibits notably superior thermal stability (405.2 °C). These ECPs are considered insensitive to mechanical stimuli (IS = 40 J, FS = 360 N) due to their compact packing and hydrogen-bonding network.

Thus, coordination polymerization is considered to be an effective approach for synthesizing next-generation EMs featuring high density and thermal stability by exploiting both existing and novel ligands that have suitable modes of coordination. Additionally, this research will further contribute to the advancement of related CP chemistry, biochemistry, and structural chemistry.

Author Contributions

Qamar-un-Nisa Tariq: investigation, experimental work, formal analysis, writing the original draft. Maher-un-Nisa Tariq: software, review & editing. Saira Manzoor: review & editing. Qiyao Yu and Jian-Guo Zhang: conceptualization, project administration, funding acquisition, supervision.

Conflicts of interest

The authors state that there are no financial conflicts of interest to disclose.

Data availability

The data supporting this article have been included as part of the ESI.†

Acknowledgements

The authors gratefully acknowledge the financial support provided by the NSFC project (22175025).

References

1 M. J. Mezger, K. J. Tindle, M. Pantoya, L. J. Groven and D. Kalyon, *Energetic Materials: Advanced Processing Technologies for next-Generation Materials*, CRC Press, 2017.
2 G. Zhang, H. Xiong, P. Yang, C. Lei, W. Hu, G. Cheng and H. Yang, A High Density and Insensitive Fused [1, 2, 3] Triazolo–Pyrimidine Energetic Material, *Chem. Eng. J.*, 2021, **404**, 126514.
3 J. Cai, C. Xie, J. Xiong, J. Zhang, P. Yin and S. Pang, High Performance and Heat-Resistant Pyrazole-1, 2, 4-Triazole Energetic Materials: Tuning the Thermal Stability by Asymmetric Framework and Azo-Bistriazole Bridge, *Chem. Eng. J.*, 2022, **433**, 134480.
4 Y. Cao, Z. Zhang, W. Lai, T. Yu, Y. Ma, Y. Liu and B. Wang, Multi-Level Structural Design Strategy toward Low-Sensitivity Energetic Materials: From Planar Molecule to Layered Packing Crystal, *Cryst. Growth Des.*, 2022, **22**(3), 1882–1891.
5 X. Xiong, X. He, Y. Xiong, X. Xue, H. Yang and C. Zhang, Correlation between the Self-Sustaining Ignition Ability and the Impact Sensitivity of Energetic Materials, *Energ. Mater. Front.*, 2020, **1**(1), 40–49.
6 A. L. Vereshchagin, Prospective Components of Rocket Propellant. I. Oxidizers, *Rev. Adv. Chem.*, 2023, **13**(3), 184–205.
7 Q.-N. Tariq, S. Manzoor, M.-N. Tariq, W.-L. Cao, W.-S. Dong, F. Arshad and J.-G. Zhang, Synthesis and Energetic Properties of Trending Metal-Free Potential Green Primary Explosives: A Review, *ChemistrySelect*, 2022, **7**(17), e202200017.
8 M. Deng, Y. Feng, W. Zhang, X. Qi and Q. Zhang, A Green Metal-Free Fused-Ring Initiating Substance, *Nat. Commun.*, 2019, **10**(1), 1339.
9 Q. Tariq, N. Un, S. Manzoor, M. Tariq, N. Un, W. L. Cao and J. G. Zhang, Recent Advances in the Synthesis and Energetic Properties of Potassium-Based Potential Green Primary Explosives, *Def. Technol.*, 2022, **18**(11), 1945–1959.
10 J. Glück, *Development and Characterization of Environmentally Benign Light and Smoke-Producing Pyrotechnical Formulations*, lmu, 2018.
11 S. M. Danali, R. S. Palaiah and K. C. Raha, Developments in Pyrotechnics, *Def. Sci. J.*, 2010, **60**(2), 152–158.

12 J. P. Agrawal, *High Energy Materials: Propellants Explosives and Pyrotechnics*, John Wiley & Sons, 2010.
13 J. Glück, T. M. Klapötke and T. Küblböck, Fine–tuning: Advances in Chlorine–free Blue–light–generating Pyrotechnics, *Eur. J. Inorg. Chem.*, 2020, **2020**(4), 349–355.
14 D. T. Bird and N. M. Ravindra, A Review: Advances and Modernization in US Army Gun Propellants, *Jom*, 2021, **73**(4), 1144–1164.
15 G. Herder, F. Weterings and W. De Klerk, Mechanical, Analysis on Rocket Propellants, *J. Therm. Anal. Calorim.*, 2003, **72**(3), 921–929.
16 W. Zhang, J. Zhang, M. Deng, X. Qi, F. Nie and Q. Zhang, A Promising High-Energy-Density Material, *Nat. Commun.*, 2017, **8**(1), 181.
17 O. T. O'Sullivan and M. J. Zdilla, Properties and Promise of Catenated Nitrogen Systems as High-Energy-Density Materials, *Chem. Rev.*, 2020, **120**(12), 5682–5744.
18 D. M. Badgujar, M. B. Talawar, V. E. Zarko and P. P. Mahulikar, Recent Advances in Safe Synthesis of Energetic Materials: An Overview, *Combust., Explos. Shock Waves*, 2019, **55**(3), 245–257.
19 N. V. Muravyev, L. Fershtat and Q. Zhang, Synthesis, Design and Development of Energetic Materials: Quo Vadis?, *Chem. Eng. J.*, 2024, **486**, 150410.
20 Q. U. N. Tariq, Y. F. Bi, S. Manzoor, M. U. N. Tariq, W. L. Cao, W. S. Dong and J. G. Zhang, Synthesis, Performance, and Thermal Behavior of Two Insensitive 3,4-Dinitropyrazole-Based Energetic Cocrystals, *Cryst. Growth Des.*, 2022, **23**(1), 112–119.
21 S. Lal, R. J. Staples and J. M. Shreeve, FOX-7 Based Nitrogen Rich Green Energetic Salts: Synthesis, Characterization, Propulsive and Detonation Performance, *Chem. Eng. J.*, 2023, **452**, 139600.
22 Q. Lang, X. Li, J. Zhou, Y. Xu, Q. Lin and M. Lu, Two Silver Energetic Coordination Polymers Based on a New N-Amino-Contained Ligand: Towards Good Detonation Performance and Excellent Laser-Initiating Ability, *Chem. Eng. J.*, 2023, **452**, 139473.
23 X. Guo, T. Liang, J. Guo, H. Huang, S. Kong, J. Shi, B. Yuan and Q. Sun, Convenient Design of Anti-Wetting Nano-Al/WO3 Metastable Intermolecular Composites (MICs) with an Enhanced Exothermic Life-Span, *Def. Technol.*, 2023, **20**, 84–92.
24 T. Wang, S. Bu, Z. Lu, B. Kuang, Z. Yi, Z. Xie, C. Zhang, Y. Li and J. Zhang, New Form of High Energy Primary Explosive: Dual Structure Composed of Ionic Salt-Based Coordination Polymers, *Chem. Eng. J.*, 2023, **457**, 141267.
25 S. Li, Y. Wang, C. Qi, X. Zhao, J. Zhang, S. Zhang and S. Pang, 3D Energetic Metal–Organic Frameworks: Synthesis and Properties of High Energy Materials, *Angew. Chem., Int. Ed.*, 2013, **52**(52), 14031–14035.
26 K. A. McDonald, S. Seth and A. J. Matzger, Coordination Polymers with High Energy Density: An Emerging Class of Explosives, *Cryst. Growth Des.*, 2015, **15**(12), 5963–5972.
27 O. S. Bushuyev, P. Brown, A. Maiti, R. H. Gee, G. R. Peterson, B. L. Weeks and L. J. Hope-Weeks, Ionic Polymers as a New Structural Motif for High-Energy-Density Materials, *J. Am. Chem. Soc.*, 2012, **134**(3), 1422–1425.
28 Y.-F. Yan, J.-G. Xu, F. Wen, Y. Zhang, H.-Y. Bian, B.-Y. Li, N.-N. Zhang, F.-K. Zheng and G.-C. Guo, Sensitive Structural Motifs Separately Distributed in Azide-Based 3D EMOFs: A Primary Explosive with an Excellent Initiation Ability and Enhanced Stability, *Inorg. Chem. Front.*, 2022, **9**(22), 5884–5892.
29 G. M. Sheldrick, *SHELXS-97, Program for Crystal Structure Solution*, University of Göttingen, Göttingen, Germany, 1997.
30 G. M. Sheldrick, *SHELXL-97: Crystal Structure Refinement Program*, Univ. Göttingen, Germany, 1997.
31 M. A. Spackman and D. Jayatilaka, Hirshfeld Surface Analysis, *CrystEngComm*, 2009, **11**(1), 19–32.
32 M. A. Spackman and J. J. McKinnon, Fingerprinting Intermolecular Interactions in Molecular Crystals, *CrystEngComm*, 2002, **4**(66), 378–392.
33 M. J. Turner, J. J. McKinnon, S. K. Wolff, D. J. Grimwood, P. R. Spackman, D. Jayatilaka and M. A. Spackman, *CrystalExplorer (Version 17.5)*, Univ. West. Aust., 2017.
34 C. B. Pinto, L. H. R. Dos Santos and B. L. Rodrigues, Understanding Metal–Ligand Interactions in Coordination Polymers Using Hirshfeld Surface Analysis, *Cryst. Struct. Commun.*, 2019, **75**(6), 707–716.
35 M. Sućeska, *EXPLO5 V6. 04*, 2017.
36 T. Wang, Q. Zhang, H. Deng, L. Shang, D. Chen, Y. Li, S. Zhu and H. Li, Evolution of Oxidizing Inorganic Metal Salts: Ultrafast Laser Initiation Materials Based on Energetic Cationic Coordination Polymers, *ACS Appl. Mater. Interfaces*, 2019, **11**(44), 41523–41530.
37 C. Zhang, T. Wang, Z. Lu, Z. Yi, B. Kuang, S. Bu, Z. Xie, Y. Li, K. Wang and J. Zhang, Keeping the Same Ratio of the Ligand and Perchlorate: Realizing the High Performance of Energetic Materials by Changing the Bonding Mode, *J. Phys. Chem. C*, 2023, **127**(27), 12923–12930.
38 C. Zhang, T. Wang, M. Xu, B. Kuang, Z. Xie, Z. Yi, Z. Lu, Y. Li, S. Zhu and J. Zhang, Regulating the Coordination Environment by Using Isomeric Ligands: Enhancing the Energy and Sensitivity of Energetic Coordination Compounds, *Inorg. Chem.*, 2023, **62**(42), 17417–17424.
39 C. Shen, Y. Xu and M. Lu, A Series of High-Energy Coordination Polymers with 3, 6-Bis (4-Nitroamino-1, 2, 5-Oxadiazol-3-Yl)-1, 4, 2, 5-Dioxadiazine, a Ligand with Multi-Coordination Sites, High Oxygen Content and Detonation Performance: Syntheses, Structures, and Performance, *J. Mater. Chem. A*, 2017, **5**(35), 18854–18861.
40 C. B. Storm, J. R. Stine and J. F. Kramer, in *Sensitivity Relationships in Energetic Materials BT - Chemistry and Physics of Energetic Materials*, ed. S. N. Bulusu, Springer Netherlands, Dordrecht, 1990, pp. 605–639.

